Fast scanning chip calorimetry study of P3HT/PC61BM submicron layers: structure formation and eutectic behaviour

Van den Brande, Niko; Van Assche, Guy; Van Mele, Bruno

Published in:
Polymer International

DOI:
10.1002/pi.5672

Publication date:
2019

Fast scanning chip calorimetry study of P3HT/$PC_{61}BM$ sub-micron layers: structure formation and eutectic behaviour

N. Van den Brande[a]*, G. Van Assche[a], B. Van Mele[a]

[a]Physical Chemistry and Polymer Science (FYSC), Vrije Universiteit Brussel (VUB), Pleinlaan 2, B-1050 Brussels, Belgium

*Corresponding author. Tel.: +32 2 629 32 77; fax: +32 2 629 32 78.
E-mail address: niko.van.den.brande@vub.be (N. Van den Brande).

Acknowledgements

The authors acknowledge the Research Foundation Flanders (FWO) for a PhD grant, the Vrije Universiteit Brussel (VUB) for a post-doctoral grant, and the foundation of public utility Hercules for financial support. TA Instruments is acknowledged for the RHC equipment.

Abstract

Fast scanning chip calorimetry was used to perform an elaborate isothermal study of P3HT/$PC_{61}BM$ sub-micron layers. The used scanning rates of 30000 $K.s^{-1}$ allow for a 'true' isothermal study, where non-isothermal effects are avoided. Results were obtained over a wide temperature range for the 1:1 composition, used in organic solar cells, and for selected temperatures for the 3:7 composition. The results can clearly be interpreted according to the eutectic behaviour expected for this system, with the 1:1 composition being enriched in P3HT and the 3:7 composition being enriched in $PC_{61}BM$. In both cases, the start of the melting trajectory corresponding to the eutectic transition coincided with the T_g of $PC_{61}BM$. This is in agreement with earlier studies that report a vitrification effect caused by $PC_{61}BM$. A bell-shaped curve of isothermal crystallization rates could be constructed for the 1:1 composition, where the T_g of the mixed amorphous phase as well as the separate components can be seen to play a role. For the 3:7 composition, clear indications are observed that a vitrified $PC_{61}BM$ phase can be formed in which isothermal crystallization takes place.

Keywords: Eutectic, P3HT, PCBM, Organic photovoltaics, Chip calorimetry

1. Introduction

An important group of organic photovoltaics (OPV) is based on the bulk-heterojunction (BHJ) concept. In such devices, the active layer is composed of donor and acceptor phases, which form a nanoscale interpenetrating co-continuous network [1,2]. The nanoscale nature of the BHJ is required for optimal performance, as the domain size should not exceed the exciton diffusion length, on the

order of 10 nm [3–5]. For this reason, understanding the complex processes that lead to morphology formation in donor/acceptor mixtures is crucial.

A benchmark system of the BHJ OPV field is the mixture of regioregular poly(3-hexyl thiophene) or P3HT as donor and [6,6]-phenyl-C_{61}-butyric acid methyl ester or $PC_{61}BM$ as acceptor. This system can reach efficiencies of 5% in a standard BHJ active layer [6], which made it the most widespread OPV active layer for some time. Although higher OPV efficiencies have been obtained by using more advanced low-bandgap donor copolymers, their synthetic complexity is much higher than that of P3HT [7], which might still make the latter a viable low-cost alternative. For this system a thermal annealing treatment is usually employed which optimizes the morphology through an interplay of several processes such as the effect of solution processing and the crystallization of donor and acceptor [6,8–12].

Several studies have already indicated that P3HT/$PC_{61}BM$ exhibits eutectic phase behaviour, apparent through the melting point depression of both components when mixed [13–18]. At the eutectic composition, both components solidify or desolidify simultaneously. This yields a fine grain morphology upon cooling, which although not a one-phase system, will desolidify upon heating at a single temperature and form again a mixed phase of eutectic composition. It is known that P3HT and $PC_{61}BM$ are miscible in the amorphous phase, while leading to separate P3HT or $PC_{61}BM$ crystals [13,15,19,20]. Different P3HT/$PC_{61}BM$ ratios can be found in literature for the eutectic composition, depending on the methodology and the P3HT used [15–17]. In most cases, the eutectic composition and melting temperature are *estimated* by extrapolation, as the actual eutectic melting is not observed. Instead, the melting enthalpies decrease as the eutectic composition is being approached. In a recent paper by our group, dedicated rapid heat-cool DSC (RHC) thermal protocols were employed, in combination with a specific solution pre-treatment and P3HT with a more narrow molecular weight distribution, in order to more accurately determine the eutectic composition and state diagram of the P3HT/$PC_{61}BM$ system [21]. For the three fractions of P3HT used in this work, the eutectic composition was always found for compositions enriched in $PC_{61}BM$ compared to the 1:1 composition by weight. A second important finding of this work was that the vitrification of $PC_{61}BM$ during cooling prevents crystallization in the mixtures close to the eutectic composition, leading to the difficult detection of the eutectic composition by conventional methods. A result of this vitrification effect is that the onset of the melting trajectory in these systems was found to coincide with the glass transition (T_g) of $PC_{61}BM$ [21].

In this work, fast scanning chip calorimetry will be employed to study 'true' isothermal structure formation (i.e. without any reordering effects that may modify the initially formed structure) in

P3HT/$PC_{61}BM$ mixtures. In earlier work, isothermal structure formation in a P3HT/$PC_{61}BM$ 1:1 mixture was studied at 127 °C (400 K), and combined with X-ray ptychography [22]. Here, a more elaborate thermal study of the 1:1 mixture will be undertaken, and isothermal structure formation in a 3:7 mixture will also receive attention.

It was found before that all non-isothermal effects in P3HT/$PC_{61}BM$ mixtures or their separate components could be avoided using heating and cooling rates of 30000 $K.s^{-1}$ [22–25]. This allowed for the construction of the bell-shaped curve of crystallization rate for P3HT thin layers. The same methodology was applied to the $PC_{61}BM$ acceptor, which was found to crystallize isothermally at temperatures as low as 370 K, over 100 K *below* its T_g as measured by chip calorimetry, which is also about 20 K *below* its T_g as measured by RHC [21,25]. The question remains whether crystallization below T_g of $PC_{61}BM$ can also occur in P3HT/$PC_{61}BM$ mixtures, as this may offer an additional explanation for the morphological instability that is sometimes observed in OPV active layers. Generally, it is thought that below the T_g no structural rearrangements can occur [19], and a higher T_g, of either the mixed phase or the components, is linked to better OPV stability [26].

2. Materials and techniques

Commercially available P3HT (Rieke Metals, $M_w = 10^5$ g mol^{-1}, $M_w/M_n = 2.4$, regioregularity ~94 %) and $PC_{61}BM$ (Solenne BV, purity 99%) were used in this study. Solutions of P3HT/$PC_{61}BM$ 1:1, and 3:7 mixtures (by weight) were prepared by dissolving a mass of P3HT and $PC_{61}BM$ into chlorobenzene, yielding a 5 wt% solution. Thin layers of P3HT/$PC_{61}BM$ were prepared on gold foil by spincoating at 100 rpm for 60 seconds, yielding layer thicknesses of about 900 nm.

The thermal study was performed using a fast scanning chip calorimeter developed at Rostock University [27,28], combined with Xensor Integration 39391 nanocalorimeter chips (60 µm x 60 µm heated area, 6-couple thermopile, two heaters). The thin P3HT/$PC_{61}BM$ layers on gold foil were placed on the active area and heated and cooled at a rate of 30 000 $K.s^{-1}$ [22–25]. The sampling methodology, using a gold foil substrate, complicates an accurate determination of the sample weight and the heat capacity. As such the obtained enthalpic data is not considered quantitative, but an accurate comparison of different isothermal treatments within the frame of this study can be made. In analogy to previous work [22–25], two different pathways to the isothermal treatment segments were used, either from the glassy state or from the molten state. The glassy state pathway is more sensitive to non-isothermal effects than the molten state one, making their comparison a suitable test to determine if non-isothermal effects were successfully avoided. All thermograms presented here correspond to heatings after an isothermal treatment and after

subtraction of a straight line in order to make small transitions more clear, without vertical shifting of the data. For all isothermal studies, a random order of short and long isothermal treatment times was used to exclude an effect of thermal history. For all measurements, the isothermal holding time at the maximum temperature was 0.01 s. By limiting the maximum temperature in the melt to 277 °C (550 K) for the study of the 1:1 mixture, any degradation of $PC_{61}BM$ was avoided [29,30], leading to a reliable and reproducible baseline and allowing for a comprehensive isothermal study. A higher maximal temperature of 357 °C (630 K) was required for the study of the 3:7 mixture, leading to accumulated degradation due to the residence time at high temperatures. Consequently, the isothermal structure formation was only studied for 117 °C (390 K) and 167 °C (440 K).

3. Results and discussion

3.1. Overview of the P3HT/$PC_{61}BM$ 1:1 mixture

The 1:1 composition of P3HT/$PC_{61}BM$ is the most ubiquitously used for OPV applications, and based on an earlier study it can be expected to be enriched in P3HT compared to the eutectic composition [21]. It can therefore be assumed that the 1:1 composition studied here is also (slightly) enriched in P3HT compared to the eutectic composition.

An interesting property of the P3HT/$PC_{61}BM$ 1:1 mixture is that the T_g step of the mixed amorphous phase can be clearly observed [22], despite the difficult detection of this transition in the separate constituents. The T_g of the mixed amorphous phase in chip calorimetry is observed at an average value slightly below 100 °C, with lower and upper limits at ca. 70 °C and 130 °C, respectively. This significantly higher value compared to the ca. 40 °C determined in bulk samples by RHC at 500 $K.min^{-1}$ [21,22], can be explained by the increased scanning rates combined with substrate effects [22–25].

A full isothermal treatment study was performed on the 1:1 composition, in a temperature interval from 7 °C (280 K) to 167 °C (440 K), utilizing pathways from the molten state and from the glassy state. Because the results for both pathways were similar, all thermograms presented here correspond to heatings after an isothermal treatment reached through the molten state pathway. Results for several selected temperatures are represented in Figure 1, and a full overview of the obtained results can be found in Figure S1.

When the endothermic peak maxima (obtained through the molten state pathway) are plotted as a function of the isothermal treatment temperature, an attempt can be made to categorize the

observed transitions according to the glass transition region (see Figure). This subdivision is more complicated than in the case of pure components [23,24] due to the interference of the glass transition region of the mixed amorphous phase *and* the pure P3HT phase. It should be noted that this plot does not attempt to identify the nature of the endothermic transitions, merely the temperature at which they are observed and the evolution over time. In order to interpret the observed peaks, the eutectic nature of the P3HT/$PC_{61}BM$ has to be taken into account.

An isothermal treatment of a 1:1 mixture, assumed to be enriched in P3HT compared to the eutectic composition, should induce several interacting phases with their respective characteristic transition temperatures: (i) a pure P3HT phase with crystals and an amorphous phase, (ii) a major eutectic phase with P3HT (nano)crystals, $PC_{61}BM$ glass, $PC_{61}BM$ (nano)crystals and a mixed amorphous phase, and eventually at longer treatment times (iii) coarsened crystals. It should be noted that the P3HT crystals formed from its pure phase are expected to correspond to form I, as form II crystals for P3HT are generally only observed for low molar mass material [31]. For this reason, the same polymorph is expected for P3HT crystals present in the eutectic.

At the highest isothermal treatment temperatures above the upper limit of the T_g region of the mixture, above 130 °C, a double endothermic peak is observed (e.g. Figure 1, D). This endothermic peak has the form of a major lower-temperature maximum, and a smaller shoulder, at higher temperatures. These can then be attributed to eutectic melting and melting of a pure P3HT phase (or delayed melting of coarsened eutectic crystals of $PC_{61}BM$ and P3HT), respectively. In agreement with earlier work both in bulk an thin layers, the eutectic melting (i.e. the onset of the melting trajectory) is found to coincide with the lower limit of the $PC_{61}BM$ T_g [21,22]. Between 50 °C and 130 °C, inside the combined T_g region of P3HT and the 1:1 mixture, the eutectic melting is the most important endothermic peak. It is a transition region, with the high-temperature shoulder still appearing at the higher temperatures, while a third peak at lower temperatures can also be observed, which is most likely enthalpic relaxation of the mixed glassy state (e.g. Figure 1, B and C). Below 50 °C, this relaxation peak becomes dominant (e.g. Figure 1, A). Note that the glass transition region of the mixed glassy state might be broadened by a low temperature tail enriched in P3HT (compositional gradient). A more detailed discussion of the eutectic melting peak with the high-temperature shoulder for the different temperature intervals can be found in the following section.

3.2. Construction of the bell-shaped curve for isothermal crystallization for the 1:1 mixture

When an isothermal treatment is performed above 87 °C (360 K) (see Figure S1), the observed endothermic peak can clearly be ascribed to the melting of crystals, despite the vitrification effects expected inside the T_g region of the P3HT and mixed phase. It seems that crystallization of the eutectic phase can occur with appearance of a high-temperature shoulder. Given the fact that $PC_{61}BM$ can crystallize as far as 100 °C below its T_g measured at 30000 $K.s^{-1}$ [25], it is fair to assume that the eutectic fine grain structure contains (nano)crystals of both P3HT and $PC_{61}BM$. For treatment temperatures of 127 °C (400 K) to 167 °C (440 K), the high-temperature shoulder forms almost simultaneous with the main peak under the form of a broad endothermic transition, while below this temperature the main peak is seemingly formed first. Note that an isothermal treatment of the 1:1 mixture, assumed to be enriched in P3HT compared to the eutectic composition, should undergo a compositional drift toward the eutectic composition induced by the initial crystallization of a minor phase of pure P3HT. The enrichment of the amorphous mixed phase in $PC_{61}BM$ toward the composition of the eutectic is seen by an increase of the initial T_g by 10 °C to 15 °C (indicated by arrows at the T_g in Figure 1, C and D, and Figure S1).

The bell-shaped curve of the isothermal crystallization rates can be constructed between 87 °C (360 K) and 167 °C (440 K). The melting enthalpies (ΔH_m) were determined after isothermal crystallization, and their evolution at different temperatures was analysed. Due to the vicinity of the two melting peaks, however, it is not possible to take into account the contributions of the different processes separately. As such, the ΔH_m determined contains contributions of the P3HT crystals formed as a pure phase, any crystals belonging to the eutectic phase structure, and coarsened crystals. Furthermore, at the earlier stages of the isothermal process, enthalpic relaxation may occur in the $PC_{61}BM$ glassy domains before crystallization of $PC_{61}BM$ below its T_g in the eutectic phase. The evolution of the ΔH_m for isothermal crystallization at three temperatures can be seen in Figure 3. These three temperatures, 87 °C (360 K), 107 °C (380 K) and 147 °C (420 K), are representative for different stages of vitrification. The treatment at 147 °C (420 K) is expected to lead to unhindered crystallization, without any interference of the T_g region of P3HT above 100 °C *and* of the 1:1 mixture above 130 °C, while treatments at 107 °C (380 K) and 87 °C (360 K) will lead to crystallization hindered by the T_g region of the mixture and by both T_g regions, respectively. It should be noted that the crystallization process is clearly much slower in all cases compared to pristine P3HT [23,24].

In analogy to the way the bell-shaped curve was determined for P3HT [23,24], the reciprocal of the time required to reach a threshold ΔH_m value of 0.02 µJ and 0.04 µJ was plotted as a function of isothermal crystallization temperature, and the obtained rates were normalized against the maximum value (found at 157 °C). For all isothermal treatment temperatures, 0.02 µJ and 0.04 µJ

are ΔH_m values in the early stages of the crystallization, but after the induction period. The results of this treatment for the results obtained through the molten state *and* glassy state pathway can be seen in Figure 4.

The rates are clearly affected by the T_g regions. A similar bell-shaped curve is obtained for both pathways, that seems to go through two local maxima at 117 °C (390 K) and 157 °C (430 K), with a minimum at 127 °C (400 K), close to the upper limit of the T_g region of the mixture. A possible explanation for such a shape lies in the enthalpy relaxation of the amorphous phase, which is expected to become more pronounced the lower the isothermal treatments are performed inside the T_g region of the 1:1 mixture, and thus may lead to an increase in the observed ΔH values. Additionally, for homopolymers the maximum of the homogeneous nucleation rate is expected in the T_g region or slightly higher, and this effect has been documented in several chip calorimetry studies where sufficiently fast rates were used to suppress crystal growth originating from heterogeneous nuclei [32]. It is very likely that a combination of these effects takes place within the complex eutectic mixture during isothermal treatments, resulting in the observed curve for isothermal crystallization rates with two maxima.

3.3. Observation of crystallization below T_g in the P3HT/$PC_{61}BM$ 3:7 mixture

So far this study has only concerned the P3HT:$PC_{61}BM$ 1:1 mixture, which is enriched in P3HT compared to the eutectic composition (P3HT excess phase), and exhibits the thermal transitions that can be expected in this case. Completely different behaviour is expected for a composition enriched in $PC_{61}BM$, as in this case a pure $PC_{61}BM$ excess phase is expected to form initially, which will co-exist with the eutectic. In order to study whether this is indeed the case, a P3HT:$PC_{61}BM$ 3:7 mixture was given the same isothermal treatment as the 1:1 mixture above.

The results of isothermal treatments at 117 °C (390 K) and 167 °C (440 K) can be seen in Figure 5. Both these isothermal treatments are below the T_g of $PC_{61}BM$ at about 200 °C, as determined by chip calorimetry in thin layers, and in the case of 117 °C the treatment also takes place below the T_g determined in a bulk sample by RHC or temperature-modulated DSC (139 °C and 131 °C, respectively) [19,21]. Two separate endothermic peaks can be observed, which can be attributed to eutectic melting, followed by the melting of $PC_{61}BM$ crystals. Again, the onset of the eutectic melting trajectory corresponds to the lower limit of the $PC_{61}BM$ T_g. When the ΔH_m evolution of these two melting peaks is plotted as a function of the isothermal treatment time, see Figure 6, an interesting evolution can be seen.

As mentioned above, a pure $PC_{61}BM$ phase is expected to form first, after which the eutectic can crystallize. Such behaviour is seen for the higher isothermal treatment, 167 °C (440 K), where a melting peak beyond 300 °C can be observed to form first followed by a peak at lower temperatures (see Figure 5, A and Figure 6, top). These endothermic peaks can therefore be attributed to $PC_{61}BM$ melting and eutectic melting, respectively. For the lower treatment temperature, 117 °C (390 K), however, the eutectic melting peak is seen first (see Figure 5, B and Figure 6, middle). Such deviation from the expected behaviour can be explained by the interference of vitrification and the glass transition temperature of $PC_{61}BM$. In fact, since both thermal treatments are performed below the T_g of pure $PC_{61}BM$, crystallization must take place inside the vitrified $PC_{61}BM$. This is an acceptable explanation for the slower observed crystallization of the excess pure $PC_{61}BM$ phase at 117 °C (390 K). The 2-step mechanism elaborated in earlier work would require the formation of an enthalpy relaxation peak first, slightly above the T_g of pure $PC_{61}BM$ [25]. This temperature of enthalpy relaxation coincides with the eutectic melting peak which is also linked to the vitrification of $PC_{61}BM$, as seen here for the P3HT:$PC_{61}BM$ 1:1 mixture (paragraph *3.1.*) and in previous work [21,22], making a separate detection of both phenomena difficult since they occur in the same temperature region. It is interesting to see that the eutectic melting peak of the 3:7 mixture is increasing with treatment time, while the relaxation peak is disappearing with the appearance of crystals for a pure $PC_{61}BM$ sample (Figure 6, bottom). At 167 °C (440 K) the crystallization of $PC_{61}BM$ from the glassy state is already fast enough so that its melting peak can be observed before the appearance of the eutectic melting. Nevertheless, these results clearly demonstrate that $PC_{61}BM$ can crystallize below the T_g of $PC_{61}BM$ in OPV mixtures.

It should be noted that the results on the P3HT/$PC_{61}BM$ 3:7 mixture are completely consistent with the eutectic phase behaviour generally expected for this system, but this is not the only phase behaviour that may give rise to such results. A tentative, alternative hypothesis involves liquid-liquid demixing for concentrations of $PC_{61}BM$ above the eutectic, instead of pure eutectic demixing. Such a miscibility gap might provide an acceptable explanation for the very steep melting point depression seen for $PC_{61}BM$ close to the eutectic. Furthermore, this can give rise to the same experimental results reported here, which were interpreted solely as eutectic behaviour.

4. Conclusion

Using the chip calorimetry methodology developed on pure P3HT and $PC_{61}BM$ thin layers it was possible to thermally characterise the P3HT/$PC_{61}BM$ 1:1 system in a layer with submicron thickness. Isothermal treatments were performed ranging from 7 °C (280 K) to 167 °C (440 K), utilizing both pathways from the molten state and from the glassy state. The observed thermal transitions

correspond to those expected for a composition which is enriched in P3HT with regard to the eutectic. The evolution of the transitions as a function of isothermal treatment temperature seems to be determined primarily by the glass transition region of the mixed amorphous phase, especially at the higher temperature side, in combination with the glass transition region of P3HT at the lower temperature side. The bell-shaped curve of isothermal crystallization rates could be constructed for temperatures from 87 °C (360 K) to 167 °C (440 K). A bell-shaped curve with two maxima was found, confirming an earlier study performed using RHC in bulk [33,34]. Interestingly, the bell-shaped curve obtained seems to be shifted about 50 K higher compared to the RHC result, a shift similar to the shift in Tg for both P3HT and the mixture. This may be the result of an important substrate effect on the mobility of the sub-micron layer. The shape of the bell-shaped curve at the lower temperature side might indicate the interference of a 2-step nucleation mechanism [3524,25]. When the mixture is treated at a temperature below 87 °C, enthalpic relaxation starts to interfere and is getting dominant at the lowest temperatures.

When a P3HT/$PC_{61}BM$ 3:7 mixture is isothermally treated, the observed thermal behaviour corresponds to that of a composition which is enriched in $PC_{61}BM$ with regard to the eutectic. An interesting result is that for the 3:7 composition, $PC_{61}BM$ was observed to crystallize well below the T_g of pure $PC_{61}BM$ even in a mixture. These findings in sub-micron P3HT/$PC_{61}BM$ layers by means of chip calorimetry provide a rationale for the chosen post-treatment temperature(s) for an optimized performance of OPV active layers and contribute to the explanation of their observed morphological instability between T_g of the mixed glassy phase and T_g of pure $PC_{61}BM$.

References

1. Huang Y, Kramer EJ, Heeger AJ, Bazan GC, *Chem Rev* **114**: 7006–43 (2014).
2. Etxebarria I, Ajuria J, Pacios R, *Org Electron physics, Mater Appl* **19**: 34–60 (2015).
3. Shaw PE, Ruseckas A, Samuel IDW, *Adv Mater* **20**: 3516–3520 (2008).
4. Gholamkhass B, Holdcroft S, *Chem Mater* **22**: 5371–5376 (2010).
5. Venkataraman D, Yurt S, Venkatraman BH, Gavvalapalli N, *J Phys Chem Lett* **1**: 947–958 (2010).
6. Ma W, Yang C, Gong X, Lee K, Heeger AJ, *Adv Funct Mater* **15**: 1617–1622 (2005).
7. Po R, Bianchi G, Carbonera C, Pellegrino A, *Macromolecules* **48**: 453–461 (2015).
8. Padinger F, Rittberger RS, Sariciftci NS, *Adv Funct Mater* **13**: 85–88 (2003).
9. Erb T, Zhokhavets U, Gobsch G, Raleva S, Stühn B, Schilinsky P, Waldauf C, Brabec CJ, *Adv Funct Mater* **15**: 1193–1196 (2005).
10. Lilliu S, Agostinelli T, Pires E, Hampton M, Nelson J, Macdonald JE, *Macromolecules* **44**: 2725–2734 (2011).
11. Shin M, Kim H, Park J, Nam S, Heo K, Ree M, Ha C-S, Kim Y, *Adv Funct Mater* **20**: 748–754 (2010).
12. Watts B, Belcher WJ, Thomsen L, Ade H, Dastoor PC, *Macromolecules* **42**: 8392–8397 (2009).
13. Stingelin N, *Polym Int* **61**: 866–873 (2012).

14. Kim JY, Frisbie CD, *J Phys Chem C* **112**: 17726–17736 (2008).
15. Müller C, Ferenczi TAM, Campoy-Quiles M, Frost JM, Bradley DDC, Smith P, Stingelin-Stutzmann N, Nelson J, *Adv Mater* **20**: 3510–3515 (2008).
16. Nicolet C, Deribew D, Renaud C, Fleury G, Brochon C, Cloutet E, Vignau L, Wantz G, Cramail H, Geoghegan M, Hadziioannou G, *J Phys Chem B* **115**: 12717–12727 (2011).
17. Li N, Machui F, Waller D, Koppe M, Brabec CJ, *Sol Energy Mater Sol Cells* **95**: 3465–3471 (2011).
18. Guilbert AAY, Reynolds LX, Bruno A, MacLachlan A, King SP, Faist MA, Pires E, Macdonald JE, Stingelin N, Haque SA, Nelson J, *ACS Nano* **6**: 3868–3875 (2012).
19. Zhao J, Swinnen A, Van Assche G, Manca J, Vanderzande D, Van Mele B, *J Phys Chem B* **113**: 1587–1591 (2009).
20. Müller C, *Chem Mater* **27**: 2740–2754 (2015).
21. Defour M, Van den Brande N, Van Lokeren L, Van Assche G, Maes W, Vanderzande D, Van Mele B, *RSC Adv* **6**: 92981–92988 (2016).
22. Van den Brande N, Patil N, Guizar-Sicairos M, Claessens R, Van Assche G, Breiby DW, Van Mele B, *Org Electron* **41**: 319–326 (2017).
23. Van den Brande N, Van Assche G, Van Mele B, *Polymer* **57**: 39–44 (2015).
24. Van den Brande N, Van Assche G, Van Mele B, *Polymer* **83**: 59–66 (2016).
25. Van den Brande N, Van Assche G, Van Mele B, *Cryst Growth Des* **15**: 5614–5623 (2015).
26. Yang X, Uddin A, *Renew Sustain Energy Rev* **30**: 324–336 (2014).
27. Zhuravlev E, Schick C, *Thermochim Acta* **505**: 1–13 (2010).
28. Zhuravlev E, Schick C, *Thermochim Acta* **505**: 14–21 (2010).
29. Larson BW, Whitaker JB, Popov AA, Kopidakis N, Rumbles G, Boltalina O V, Strauss SH, *Chem Mater* **26**: 2361–2367 (2014).
30. Maibach J, Adermann T, Glaser T, Eckstein R, Mankel E, Pucci A, Mullen K, Lemmer U, Hamburger M, Mayer T, Jaegermann W, *J Mater Chem C* **2**: 7934–7942 (2014).
31. Brinkmann M, *J Polym Sci Part B Polym Phys* **49**: 1218–1233 (2011).
32. Schick C, Androsch R, Schmelzer JWP, *J Phys Condens Matter* **29**: 453002 (2017).
33. Demir F, Van den Brande N, Bertho S, Voroshazi E, Manca J, Vanderzande D, Heremans P, Van Mele B, Van Assche G, In *Proceedings of the SPIE*, B. P. Rand, , C. Adachi, and V. van Elsbergen, Eds.; (2012); 84350V.
34. Demir F, Vrije Universiteit Brussel, (2014).
35. Vekilov PG, *Cryst Growth Des* **10**: 5007–5019 (2010).

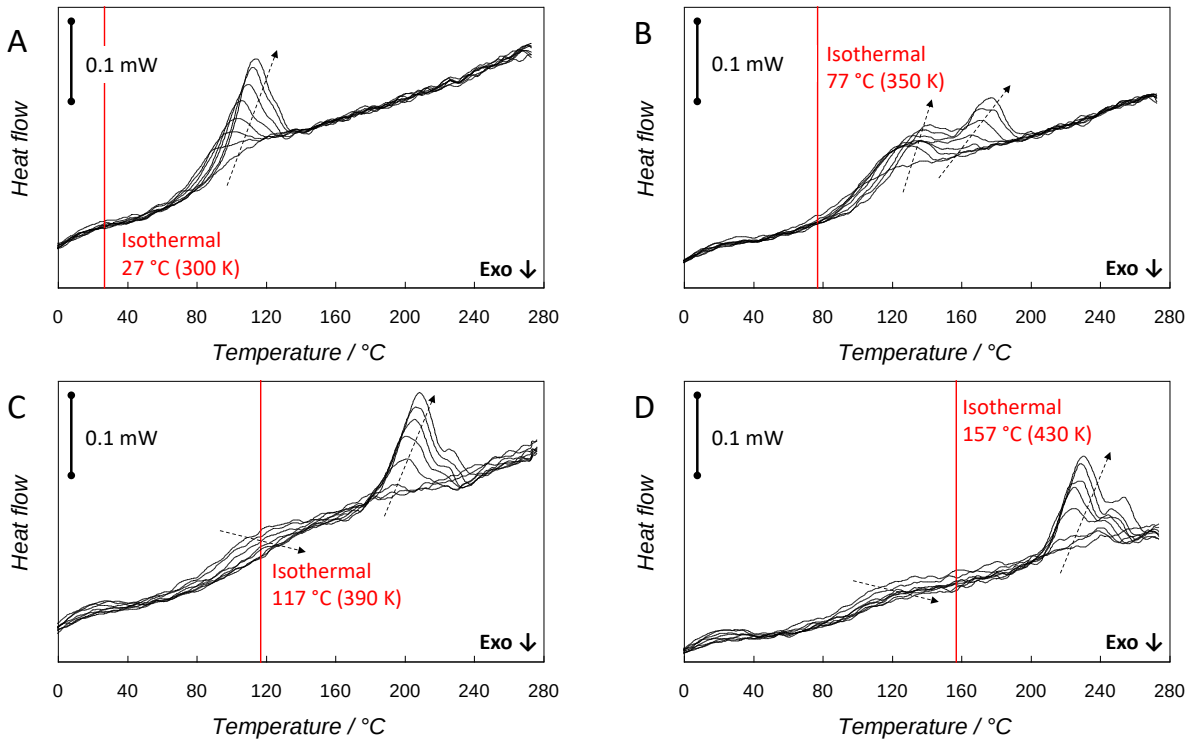

Figure 1: Evolution of P3HT/$PC_{61}BM$ 1:1 transitions during heating at 30000 $K.s^{-1}$, formed by isothermal treatments at 27 °C (300 K, A), 77 °C (350 K, B), 117 °C (390 K, C), and 157 °C (430 K, D). Results are shown for isothermal treatments of 0 s, 2.6 s, 10.5 s, 42.9 s, 176 s, 721 s, 2952 s, and 7556 s. Arrows have been drawn to clarify observed trends in the thermal transitions.

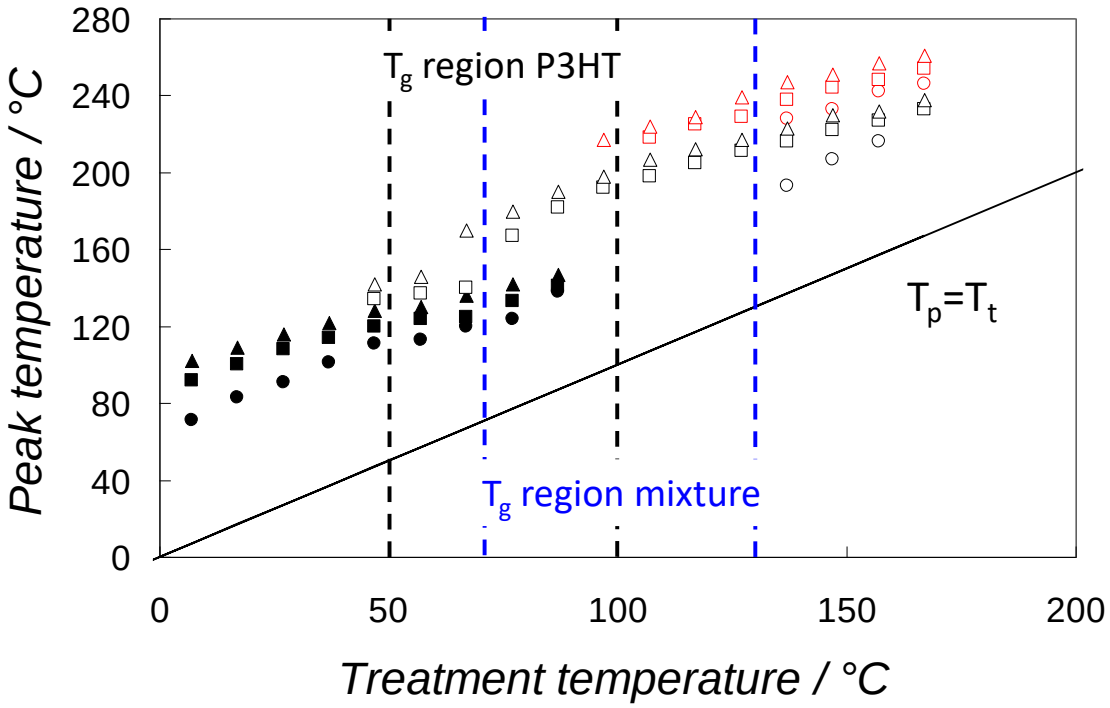

Figure 2: Endothermic peak maxima (T_p) of P3HT/$PC_{61}BM$ 1:1 mixture as a function of the isothermal treatment temperature (T_t) for the whole temperature range studied, using the molten state pathway. The enthalpic relaxation peak (solid symbols), eutectic melting peak (open symbols) and the high-temperature shoulder (red open symbols) are plotted. Peak temperatures were plotted after isothermal treatment times of 2.6 s (circles), 176 s (squares), 7556 s (triangles). The $T_p=T_t$ line as well as the T_g zones for pure P3HT and the mixture are shown for comparison.

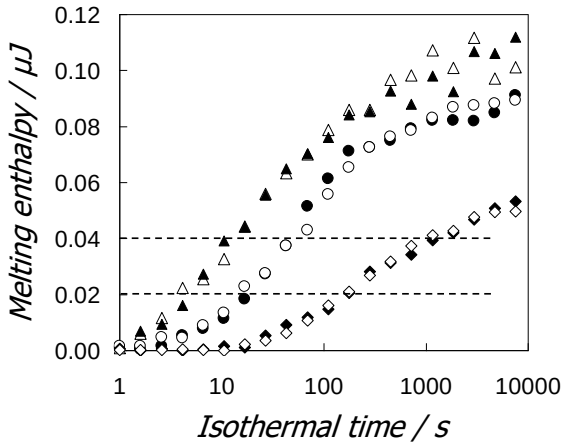

Figure 3: Evolution of P3HT/$PC_{61}BM$ 1:1 melting enthalpies by isothermal crystallization at 87 °C (360 K) (diamonds), 107 °C (380 K) (circles) and 147 °C (420 K) (triangles) obtained at scanning rate of 30000 $K.s^{-1}$, with results from molten (filled symbols) and glassy state (open symbols). The dashed lines indicate the threshold values of melting enthalpy (see text).

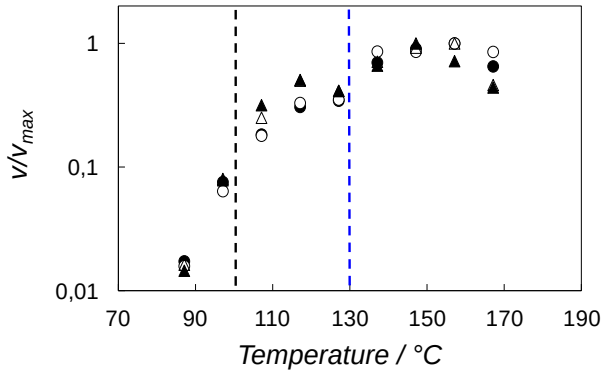

Figure 4: Isothermal crystallization rates for P3HT/$PC_{61}BM$ 1:1 in the interval from 87 °C (360 K) to 167 °C (440 K) calculated as the reciprocal of a threshold time for crystallization, divided by the maximum rate at 157 °C (430 K) (see text). Results are given for the pathway from molten (filled symbols) and glassy state (open symbols) for both threshold values of 0.02 µJ (circles) and 0.04 µJ (triangles). The upper limits of the T_g region of P3HT (100 °C, black line) and the mixture (130 °C, blue line) are indicated.

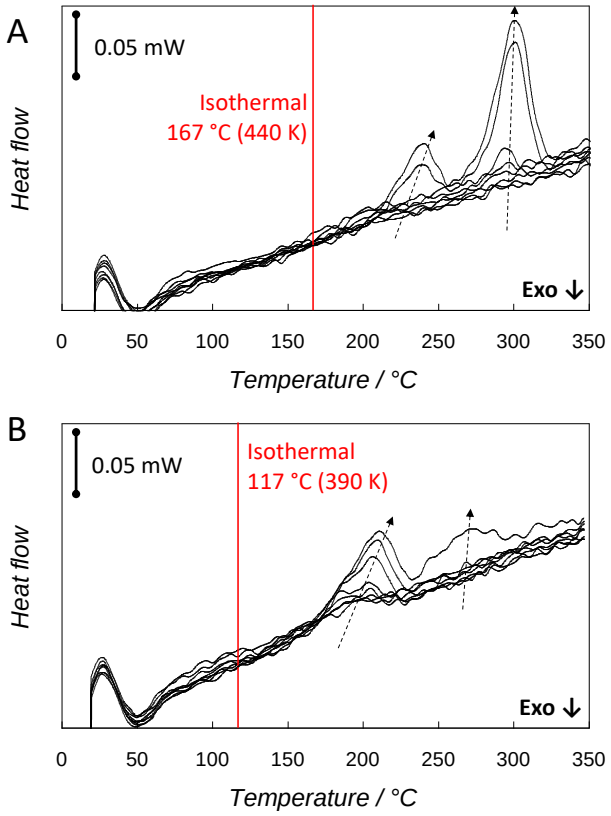

Figure 5: Evolution of P3HT/$PC_{61}BM$ 3:7 transitions during heating at 30000 $K.s^{-1}$, formed by isothermal treatments at 167 °C (440 K, A), and 117 °C (390 K, B). Results are shown for isothermal treatments of 0 s, 2.6 s, 10.5 s, 42.9 s, 176 s, 721 s, 2952 s, and 7556 s. Arrows have been drawn to clarify observed trends in the thermal transitions.

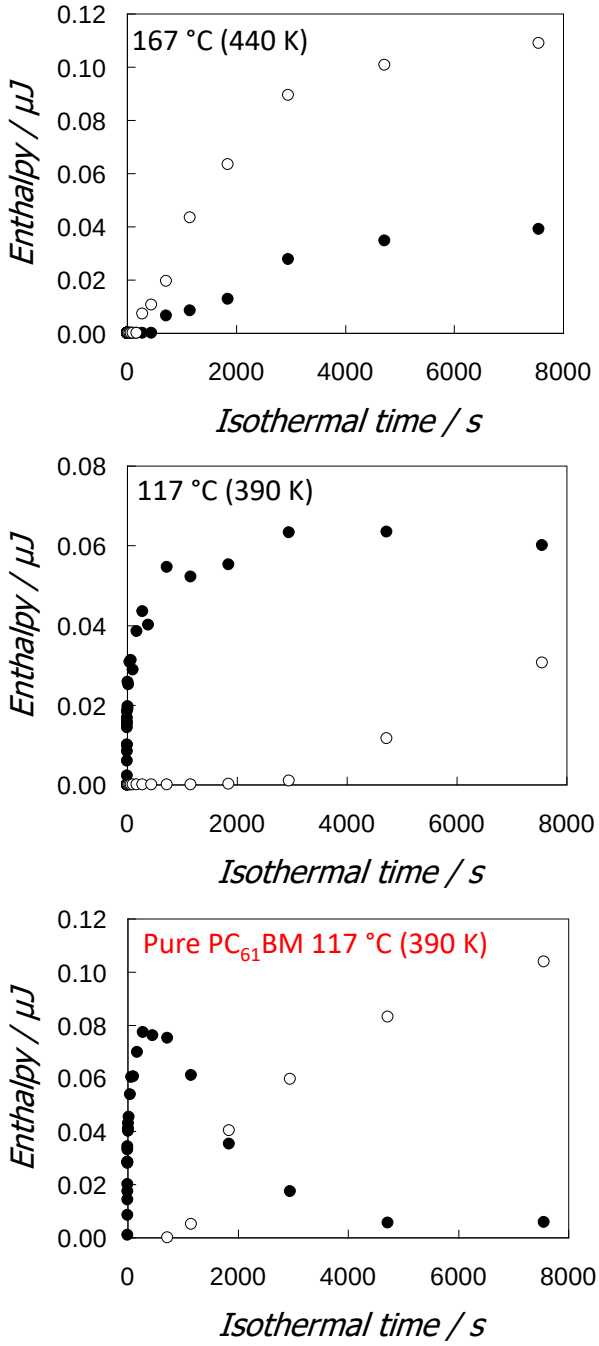

Figure 6: Evolution of the melting enthalpy of the eutectic melting peak (solid symbols) and the $PC_{61}BM$ excess phase (open symbols) for the P3HT/$PC_{61}BM$ 3:7 mixture during an isothermal treatment at 167 °C (440 K) (top) and 117 °C (390 K) (middle). For comparison the evolution of enthalpic relaxation (solid symbols) and melting enthalpy (open symbols) during an isothermal treatment at 117 °C (390 K) is also shown for a pure $PC_{61}BM$ sample (bottom) [25].